JOURNAL OF MATERIALS SCIENCE 18 (1983) 1852–1862

Fatigue crack growth rates for very short cracks developing at fastener holes in 7075 and 7010 aluminium alloys

P. J. E. FORSYTH
Materials Department, Royal Aircraft Establishment, Farnborough, UK

P. M. POWELL
Mechanical Engineering Department, University of Southampton, Southampton, UK

Fatigue crack growth rates have been determined for very short corner and bore cracks developing from fastener holes. This was made possible by the use of a simple load programme which provided a contrasting fracture feature or marker. The programme consisted of a high–low–high switch of load ratio (R) usually in blocks of 100 loads. A constant $\Delta\sigma$ was maintained within each block. The crack growth rate data for short cracks was in reasonable agreement with the published long crack data for 7075 and 7010 alloy. Strong retardation effects were in evidence and certain features of the fractures shed new light on the retardation models, and also on those of fatigue fracture itself.

1. Introduction

The growing application of the American damage tolerance design requirements specification [1] is a reflection of the engineer's concern for the dangers that arise when manufacturing defects appear at fatigue critical points in his design.

This specification requires that initial defects arising from manufacturing practice, including material flaws, shall be assumed to exist at all fatigue critical points in the design, and that the fatigue design of the part must take this into account. Thus available fatigue life is reduced to that for crack growth from the specific size defect to a depth defined by limit load requirements and a factor for scatter in the population. In many cases a considerable proportion of the usable crack life will be consumed in the "short crack" phase, < 2 mm, and it is now, more than ever, essential to study the behaviour of these short cracks in terms of their developing shapes and associated growth rates. Furthermore it is important to examine the contribution of metallurgical variables as well as retardation etc., in this same context.

The only feasible way to do this is by post-fracture observation. In the above mentioned circumstances crack growth rates will be extremely small, may be as low as 10^{-6} mm cycle^{-1}, and no observational technique will detect or resolve striations, even if such features were to be produced at all under such conditions. This problem can be largely overcome by using a repeating load programme that produces a more coarsely spaced feature on the fracture, rather like a wave with superimposed minor ripples (individual striations) on its surface. This is a somewhat different approach to the normal one where single heavy loads are introduced at regular intervals to act as markers.

This paper describes work done on holed 7075-T7351 and 7010-T7651 aluminium alloy fatigue specimens where crack growth rates for very small cracks, down to 0.1 mm, have been determined fractographically. Retardation and acceleration effects have been observed and a model describing the mechanism has been proposed.

2. Experimental details

2.1. Materials

The 7075 aluminium alloy was received as 25 mm rolled plate in the T7351 heat-treated condition.

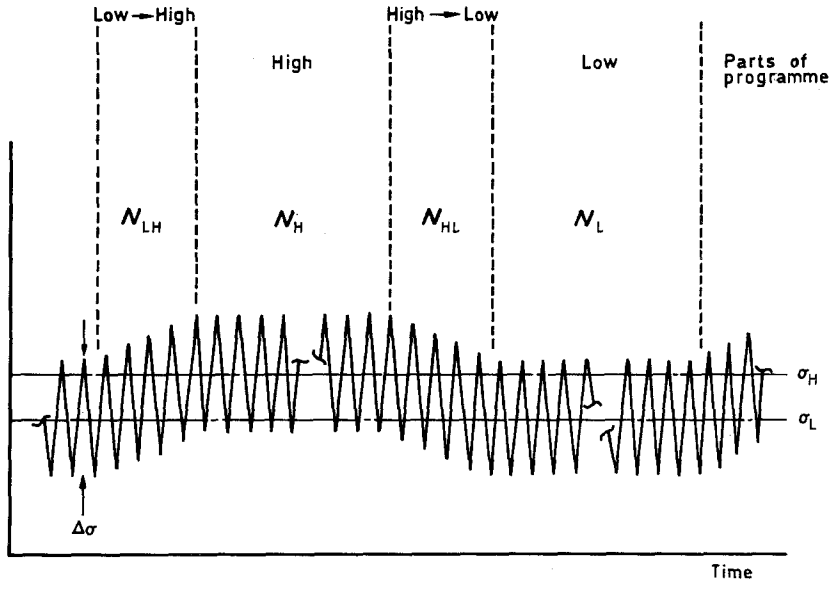

Figure 1 Diagram showing loading sequence used for this work. The numbers were, generally, $N_H = 100 = N_L$, $N_{LH} = 10 = N_{HL}$.

Its chemical composition was as follows:

	Zn	Mg	Cu	Cr	Fe	Si	Ti	Al
(%)	5.47	2.54	1.35	0.18	0.17	0.12	0.03	balance

The 7010 alloy was supplied to DTD 5120 specification, i.e. it was in the T7651 heat treated condition.

Its chemical composition was as follows:

	Zn	Mg	Cu	Zr	Fe	Si	Mn	Al
(%)	6.28	2.45	1.74	0.13	0.09	0.12	0.02	balance

The heat treatment condition for the two alloys represents different degrees of overageing, both applied to confer some degree of stress corrosion resistance, the T73 temper being more overaged and, therefore, nominally more resistant than the T76 temper. Both alloys had a similar hardness (about 170 Hv) and also similar grain sizes (about 25 μm).

2.2. Fatigue crack propagation test pieces

The test piece used for the 7075 work was a rectangular coupon 178 mm long × 32 mm wide × 6.4 mm thick containing a central 6.4 mm diameter hole. The test pieces were always oriented longitudinally with respect to the rolling direction.

The standard of hole manufacture was controlled to minimize variability of the surface working in the bore, being machined to the following procedure based on an AGARD specification for a high quality finish:

(i) Drill 3 mm pilot hole.

(ii) Open up hole with 6 mm drill at 2700 rev min^{-1} with a feed rate of 0.08 mm rev^{-1}.

(iii) Finish hole with 6.4 mm (0.25 inch) reamer at 1500 rev min^{-1} with a feed rate of 0.20 mm rev^{-1}.

Test pieces were polished in the longitudinal direction on 600 grade silicon carbide paper prior to testing; this procedure removed any burrs from the hole, while maintaining a sharp corner.

The 7010 test pieces were waisted test pieces 25 mm wide at the critical section and 5 mm thick. They were then subjected to the same drilling and finishing procedures.

2.3. Fatigue testing

The fatigue crack propagation tests were conducted on a 250 kN MAND servo hydraulic machine, operating under load control at a frequency of 10 Hz. The machine was equipped with a ramp generator and hold-level facility, which enabled a trapezoidal waveform to be applied to the test piece; the sinusoidal load at 10 Hz was superimposed on this wave form to give a simple programme in which a cyclic load of constant amplitude was applied in blocks that alternated with high and low mean loads as shown in Fig. 1.

TABLE I

Test No.	Cyclic stress $\Delta\sigma$ (MPa)	Mean stress		Stress ratio		Number of cycles in programme				Programmes to failure	Crack depth range studied	
		σ_L	σ_H	at σ_L	at σ_H	Total N_p	N_L	N_H	$N_{LH}=N_{HL}$		a_{min} (mm)	a_{max} (mm)
7075-T7351												
1	90	60	90	0.14	0.33	224	100	100	~12	23775	0.36	2.04
2	90	60	90	0.14	0.33	224	100	100	~12	605	0.08	1.73
3	90	60	90	0.14	0.33	209	100	95	~7	588	0.21	3.11
4	90	60	90	0.14	0.33	214	100	100	7	9900	0.21	1.33
5	90	60	165	0.14	0.57	244	100	100	22	600	0.05	0.51
6	90	90	165	0.33	0.57	234	100	100	17	485	0.18	2.37
7	90	55	75	0.10	0.25	212	100	100	6	4800	0.13	4.16
7010 (DTD 5120)												
1	90	60	90	0.14	0.33	220	100	100	10	1000	0.42	2.29
2	80	53.3	79.9	0.14	0.33	216	100	100	8	1650	0.16	1.81
3	90	60	90	0.14	0.33	218	100	100	9	615	0.10	3.97

The cyclic stress range $\Delta\sigma$ and the low and high mean stresses σ_L and σ_H in each test are listed in Table 1. The change in the mean stress level could not be abruptly applied, but the change occurred over a period of about 10 cycles, indicated as the periods N_{LH} and N_{HL} in Fig. 1. The number of cycles in the ramp varied somewhat for the different test conditions used but could be accurately monitored.

Each complete load programme consisted of approximately 220 cycles, approximately 100 at each mean stress level and 10 each for the up and down ramps. At a later stage in the work, the numbers of cycles in the blocks were changed to study the extent of the retardation zones observed. Constant amplitude tests have also been done at R ratios of 0.14, 0.33 and 0.57.

2.4. Fractographic techniques

Fractures were examined using optical microscopy up to x 600; suitable areas of each fracture were located using the stage micrometers of the microscope so that each area was located by two measurements, (i) the distance from the bore of the hole, x, and (ii) the distance from the test piece surface, y. The fine scale division on the micrometers was 10 μm. The spacing of the programme marks was measured on photographs to 0.1 μm. When a number of similar programme marks were observable on one facet, the average spacing was calculated and the distances x and y measured to the centre of the facet. Fractures were also examined by scanning electron microscopy using similar measuring methods.

At stress intensity levels where individual striations became resolvable the growth rate data could be supplemented by measuring their spacings. This was particularly valuable because in these circumstances the wave feature is so spread as to become difficult to detect.

3. Results

3.1. Test lives

The form of the block loading described, where $\Delta\sigma$ is maintained constant but the R ratio is repeatedly switched, produced clearly observable programme markings that have been successfully "read" down to <0.05 mm crack depth. The underlying mechanisms whereby this marking is produced on the fracture surface will be described later in this paper. Table I summarizes the conditions used for the various tests and gives total lives achieved in terms of the programmes represented by a complete two block cycle. It can be seen that, for similar loading conditions, a large scatter in life was experienced, for example on 7075-T7351 lives ranged from 23775 programmes down to 588.

3.2. Crack growth details – location and shape of cracks

In the majority of cases the fatigue crack propagated from one side of the hole; the fatigue fracture at the other side of the hole usually extended less than 1 mm from the bore and the fracture of this section was predominantly of a single slant, tensile nature.

This behaviour may have been caused by slight non-axiality in loading whereby a small, tensile bend stress would have been superimposed on one

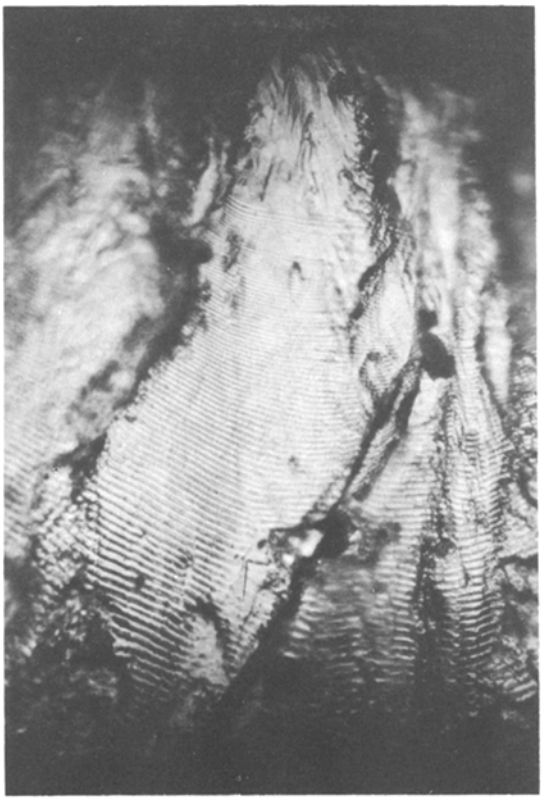

Figure 2 Programme markings outlining the front of expanding cracks (optical fractographs) 7010 aluminium alloy. Various fatigue origins arrowed A. Magnfication × 528.

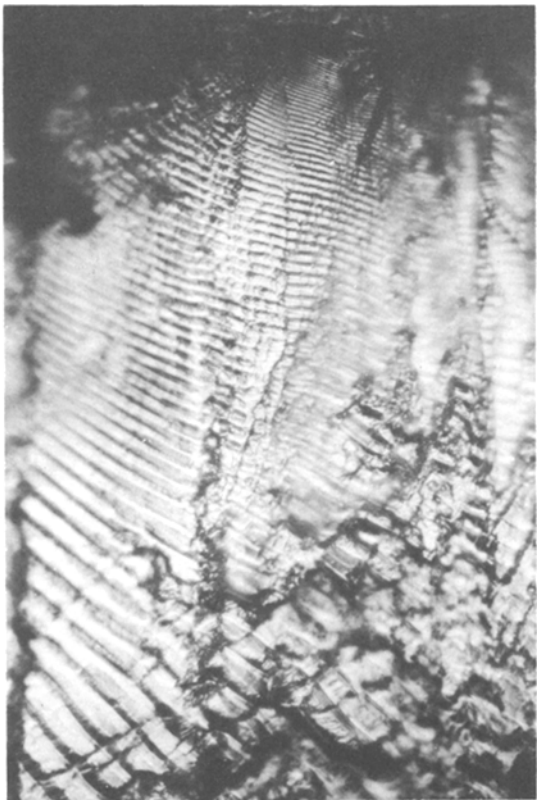

Figure 3 First clearly visible programme marks B, but resolution possible to about 12 μm from origins at some places. Programme $N_H = 8$, $N_L = 2387$, $N_{HL} = 14$. Magnification × 528.

side of the hole, which then became the preferred site for cracking. However, a universal joint was present in the loading train and non-axiality would have been virtually eliminated. A more likely reason is that the crack initiation and early growth occupied the major part of the test; consequently, when a crack started from a microstructural or machining defect at one side of the hole, it could have propagated across that section before an origin had been exploited at the opposite side.

In the 7075 alloy, where the specimens were 6.4 mm thick, two of the specimens had crack origins in the bore of the hole (2.3 and 1.2 mm from the nearest corner in tests 2 and 3, respectively) while in test 1, the abnormally long life one, there was a corner crack. The bore cracks were semi-elliptical, but were considered as semi-circular for the calculation of ΔK. In all cases the changing shape of the crack with depth could be clearly seen from the marking pattern. Figs. 2, 3 and 4 show examples of this. It was also frequently observed that cracks were retarded in their growth in the bore region, i.e. the crack front swept forward just beneath the bore surface.

3.3. Programme marks at long crack lengths and comparison with short crack markings

At crack depths of between 8 and 12 mm from the bore of the hole it was possible to identify and count the individual load striations. The complete programme marking, at this stage would be 120 to 220 μm. The two step levels could be identified and also an anomalously high acceleration in the transition ramp where the low → high stress change took place. No feature could be observed that related to the high → low change. Fig. 5 shows a complete programme in 7075-T7351 where the 100 high R ratio cycles can be counted. At a greater crack depth the 100 low level cycles could also be counted. For reasons that will be described later, the two R ratio levels could be separated in terms of the crack extension, i.e. the damage, at both the high level (where individual striations

Figure 4 Programme markings outlining the front of a growing fatigue crack in 7010 aluminium alloy. Note microstructural influence on fracture topography (optical fractograph). Programme $N_H = 100 = N_L$, $N_{LH} = 10$. Magnification × 232.

were resolvable) and at low level where an abrupt fracture plane change occurred between the blocks. Thus the relative contribution of each block could be determined throughout the whole range of the crack depth examined. This was found to be a constant ratio irrespective of the crack depth and it soon became obvious that the low R ratio period was subject to powerful retardation from the previous high level block. No variation in the growth rate could be determined within either the low or high level blocks, the striation spacings being remarkably constant.

Some of the retardation factors have been about 8 to 1 when compared with the constant amplitude data. The Pearson [2] modification of the Forman equation gave the best fit to the constant amplitude data, but only predicted a 1.6

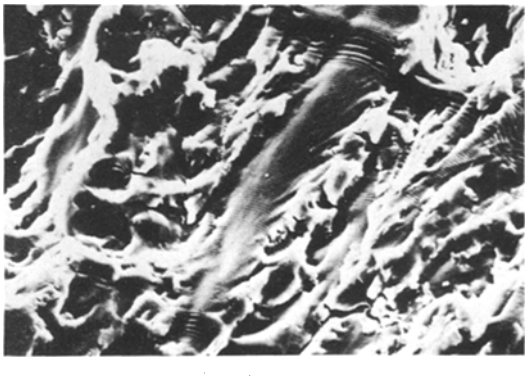

Figure 5 Individual high level striations A, low level block still not resolved B, coarse transition striations, C (scanning electron micrograph). Programme $N_H = 100 = N_L$, $N_{LH} = 10$. Magnfication × 580.

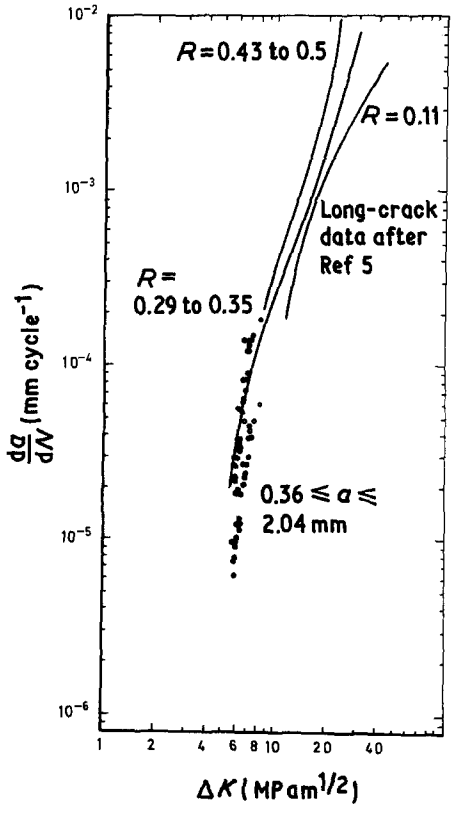

Figure 6 Fractographically obtained fatigue crack growth data for 7075-T7351 Test No. 1. Fracture data: $R = 0.14$, ○; $R = 0.33$, ●. ΔK: Newman's solution, corner-crack.

effect for an R ratio change where a 20:1 effect had been observed in practice. Thus the retardation observed was real and no absolute crack growth data against ΔK could be obtained by the method.

3.4. Fatigue crack growth data

The fractographically determined fatigue crack growth data for these small cracks is summarized in Figs. 6 and 11, superimposed on ESDU curves [3], where these are available. The calculation of ΔK has been based on various solutions [4].

Each striation or programme mark count gives the high and the low block growth rates either directly where individual striations can be seen or by the ratio of the two parts of the programme mark where they are not directly resolvable. Thus the points at each high and low R ratio determination are paired. The retardation effects can be seen by inspection of the data and comparison with the constant amplitude curves. The retardation effects for two overload ratios are given in Table II.

As there was no evidence that the low block crack was emerging from the retardation zone,

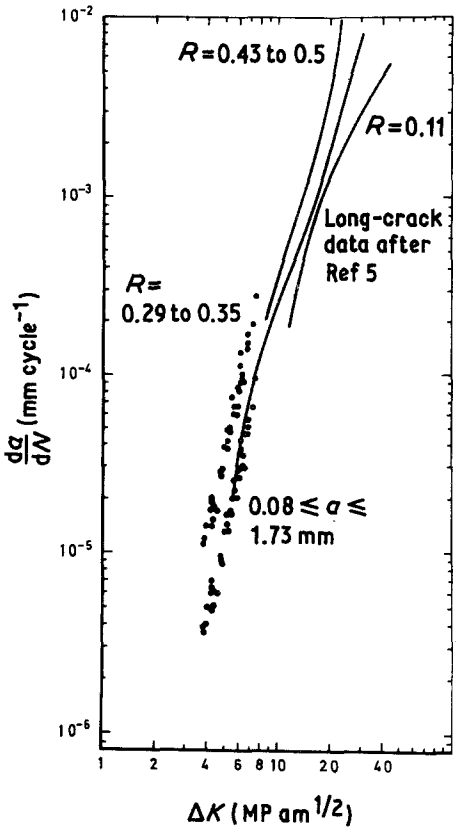

Figure 7 Fractographically obtained fatigue crack growth data for 7075-T7351 Test No. 2. $R = 0.14$, ○; $R = 0.33$, ●. ΔK: solution for semicircular surface crack.

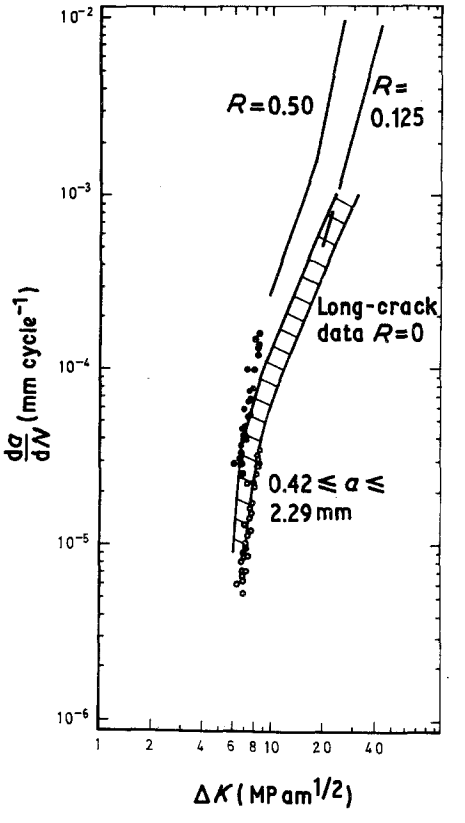

Figure 8 Fractographically obtained fatigue crack growth data for 7010 (DTD 5120) Test No. 1. $R = 0.14$, ○; $R = 0.33$, ●. ΔK: solution for corner crack.

such as an increase in striation spacing with time, higher numbers of cycles in the low level blocks were tried, up to 2500 cycles. The result of this was to further increase the retardation, up to 40 times, indicating that the effect was, in fact, increasing with depth as has been reported in other work [5]. This is now a direct indication that such retardation effects, even the build up to maximum, are locally observable and are not, therefore, macroscopic crack front rearrangements.

4. Discussion

4.1. A description of the programme markings

Previous work had indicated that periodically changing the mean of repeated loads would provide a satisfactory marker, but it was still somewhat surprising how clearly the programme used in this work revealed itself on the fracture surface, even with the quite small changes in load ratio that were initially used.

TABLE II

Specimen	Load ratio R		Peak overload ratio	Effect of R (Forman)	Effect of R (Pearson)	Constant amplitude tests. Effect of R	Retardation* ratio as measured by fractography
	σ_L	σ_H					
Nos. 1–4	0.14	0.33	1.3	1.4	1.2	0	3
7075-T7351 No. 5	0.14	0.57	2	2.6	1.6†	1.6	8

*Measured against equivalent R ratio constant amplitude growth rate.
†Calculated for a $K_c = 66$ MPa m$^{1/2}$ and $\Delta K = 10$ MPa m$^{1/2}$.

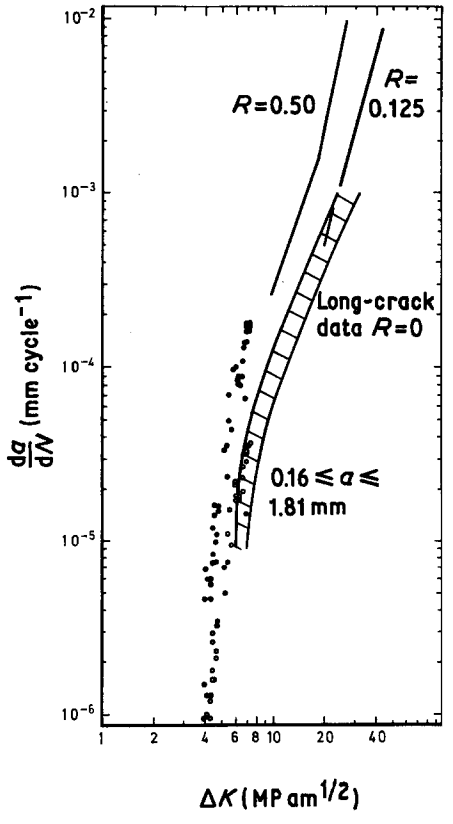

Figure 9 Fractographically obtained fatigue crack growth data for 7010 (DTD 5120) Test No. 2. $R = 0.14$, ○; $R = 0.33$, ●. ΔK: solution for corner crack.

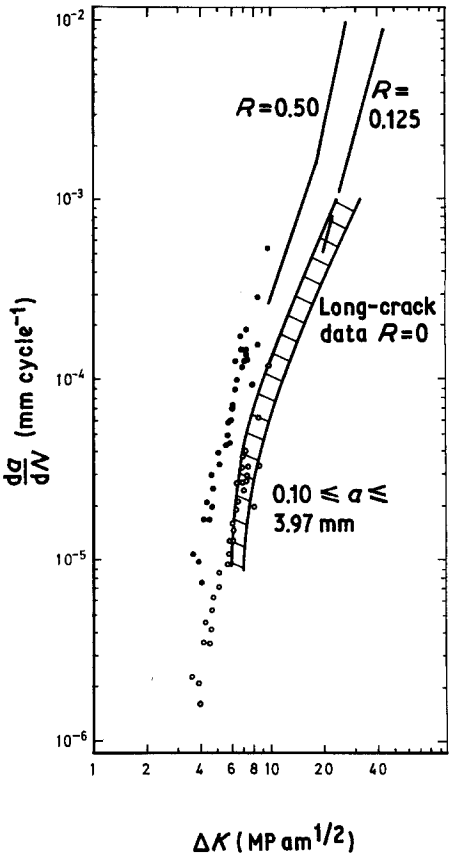

Figure 10 Fractographically obtained fatigue crack growth data for 7010 (DTD 5120) Test No. 3. $R = 0.14$, ○; $R = 0.33$, ●. ΔK: Newman's solution for corner crack.

It is of interest to consider, in some detail, what is happening at the fatigue crack tip to produce the contrast necessary to reveal the bands. An inspection of these markings, as shown in Figs. 12 and 13, shows that this contrast is derived from two distinct topographical features:

(i) a wave profile on the fracture surface, and

(ii) the presence of "cliffs" or hackle (in glass fracture terminology) developing at right angles to the crack front during the lower load ratio growth.

The optical microscope can be very sensitive to surface angle changes and assuming adequate resolution in the first place the contrast from a wave-like profile increases dramatically as the numerical aperture is reduced.

It is clear that for a given wave height, the longer the wavelength the less contrast will be available from the lost reflected light. In the present examples most of the contrast is obtained from the steeper front profiles or escarpment that develops on the low → high ramp of about 10 cycles, but from the point of view of counting these markings it is also an advantage to have as close a spacing as possible, assuming adequate resolution. The spacing is dictated mainly by the number of loads in the high block and the 100 chosen for most of this work is about right for convenience of measurement down to about 10 μm crack depths as shown in the optical fractograph in Fig. 14. In this particular respect there is little to be gained from scanning electron microscopy, although the extra resolution and depth of focus becomes more valuable for resolviing individual striations at greater crack depths.

Having defined the two features that provide contrast and are also, to a degree separately identifiable with the different phases of the programme, it is necessary to consider their significance in terms of:

(i) the retardation effect, and

(ii) the fatigue crack growth mechanism itself.

These two aspects are dealt with in the following sections.

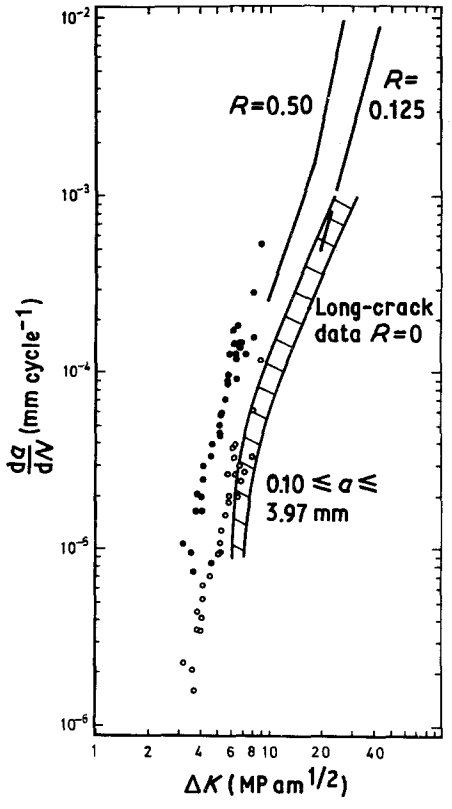

Figure 11 Fractographically obtained fatigue crack growth data for 7010 (DTD 5120) Test No. 3 continued. $R = 0.14$, ○; $R = 0.33$, ●. ΔK: Newman's solution corner crack.

4.2. Model for retardation

As has been described, the block of high loads have always produced a uniform set of striations, the spacing of which is generally characteristic of the long crack growth rates for the same loading conditions. This suggests that there is a negligible interaction in the low → high sequence, with the exception of the transition phase mentioned in an earlier section. However, when the high → low sequence occurs, which passes through a descending ramp of about 10 cycles, the crack growth rate reduces abruptly with no influence from these transition cycles. This abrupt change in rate is accompanied by an immediate change in surface tilt. In this respect the high load block plane is generally normal to the assumed maximum principal tensile stress and the low block tilts away from this plane at some angle, which can be as high as 30°, but may be much smaller. This somewhat tilted fracture phase is also characterized by the appearance of hackle or "cliff" edges. This hackle is a characteristic feature of fatigue fracture in most metals and of brittle fracture in other substances, and will be discussed in detail in the next section. It is sufficient to say, at this stage, that inasmuch as the low block growth rates are heavily retarded, and may be one-fortieth of the adjacent high rate period, it is to be expected that the hackle, which in this context seems to be a low growth

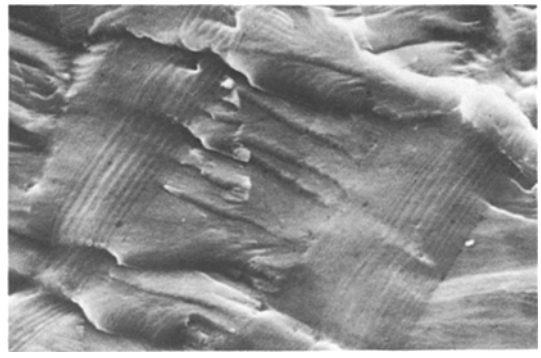

Figure 13 Detail of hackle features and ramp striations in 7010 aluminium alloy. Programme $N_H = 8$, $N_L = 2387$, $N_{HL} = 14$. Magnfication X 174.

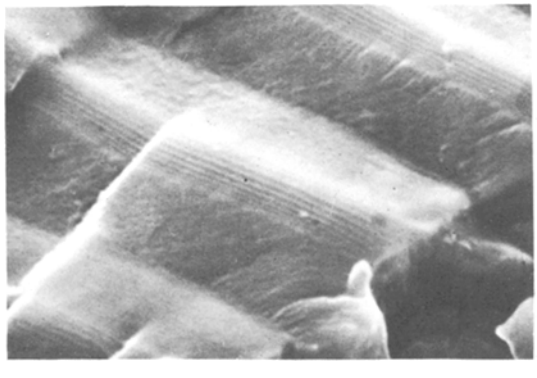

Figure 12 Fatigue fracture in 7010 alloy showing wave profile and hackle features. Magnification X 4060.

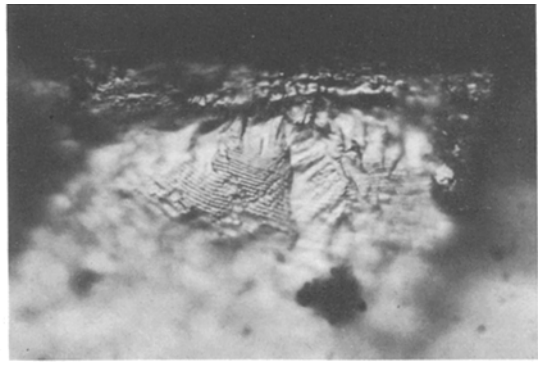

Figure 14 First observable striations at about 10 μm from the fatigue origins. Magnification X 870.

rate phenomenon, will be confined to these zones. However, because the cliff edges set up considerable jogs along the crack front, these steps are not immediately "washed out" when the load is increased, and the cliff edge may persist through part or all of the high block crack extension zone. There is also some evidence that the first few high level cycles can tear or somehow accentuate the cliff edge back into the low level growth zone.

There has been no evidence that the crack in the low block phase has started to emerge from the retardation zone set up by the previous high block loads and, as mentioned in an earlier section, this retardation increases as the crack extends and the full range of the effect has, as yet, not been fully explored.

Perhaps the acceleration of the crack through the low → high transition is the most revealing phenomenon with regard to defining a retardation model. This behaviour strongly suggests that a fairly local resistance zone is set up by the crack itself and an increase in the stress intensity factor causes an immediate acceleration as the zone of resistance is penetrated and destroyed. This more highly loaded crack now quickly forms (< 5 cycles) a new crack resisting zone of its own which, presumably, because the stress is higher extends more deeply ahead of the crack tip. The evidence suggests that this zone, which must be highly strained, contains some dislocation arrangement which is dynamically stable to its own stress input. The zone must move forward with the advancing crack tip, but is not catastrophically penetrated by the crack unless the stress is raised. In all of this work $\Delta\sigma$ has been maintained constant, thus all of these effects must be related to σ_{max}. It is clear that such a zone, if stable to its own crack tip stress, will be difficult to penetrate by any crack with a reduced K_a. Such local reproducible effects, as these, can only be explained in terms of crack tip condition and cannot be related to crack closure effects that would be erratic and unequally distributed around the crack front.

4.3. Model for fatigue crack tip extension and associated features

The use of a loading programme that has produced systematic changes in the tilt of the fracture plane has enabled certain deductions to be made about the basic mechanism of crack extension. The obvious association of the hackle feature with low crack growth rates is more strikingly demonstrated in the programme loaded specimens than in constant amplitude fatigue fractures where the change in K_{max} with crack depth is gradual.

Both of these features, tilt and steep cliffs or hackle, can be shown by selected area matching and other characteristics, to fit hill to valley, thus showing that, on a coarse microscopic scale, the crack is extending with deviations of the plane rather than by symmetrical opening strains. Furthermore, closer examination of individual load striations confirms the earlier observations of Stubbington [6], that these too fit hill to valley. The symmetrical opening mode of crack extension that has formed the basis of so many of the models in the literature on this subject does not happen in the commercial alloys used for this work. It is now clear that, just as the coarse plane tilts are the result of a changing load level in the programme so the actual load level in the individual cycle changes the crack angle on the smaller scale.

The crack opening displacement (COD), as calculated from the following equation, $\delta = G/\sigma_y$, is generally at least an order of magnitude greater than the wave height of the striations. In one specific instance the COD was calculated at 6.7 μm under conditions where the local crack extension distance/cycle, i.e. the striation spacing, was 1 μm, with an estimated wave height of < 0.5 μm.

It is tempting to relate fracture surface tilts entirely to crystallographic influence and this is experienced in cases where cracks change from stages I to II, but in the present work all of the local crack interactions seem to relate to continuum behaviour and some may even be predicted from fracture mechanics considerations. Thus we see a contribution from linear elastic behaviour together with modifications resulting from continuum plasticity with no defined predominant crystal plane. A good example of this is the development of hackle fracture and the dramatic reduction of this feature when the load is suddenly increased.

This behaviour can be explained if one considers that at low growth rates a number of individual segments of the same general crack front extend forward one increment as the load is applied, initially from discrete points, but extending sideways until they approach and interact with their neighbours. Such segments are unlikely to be perfectly co-linear and their tips may approach and even slightly pass above or below their neighbours' tips. The stress intensity solutions for such

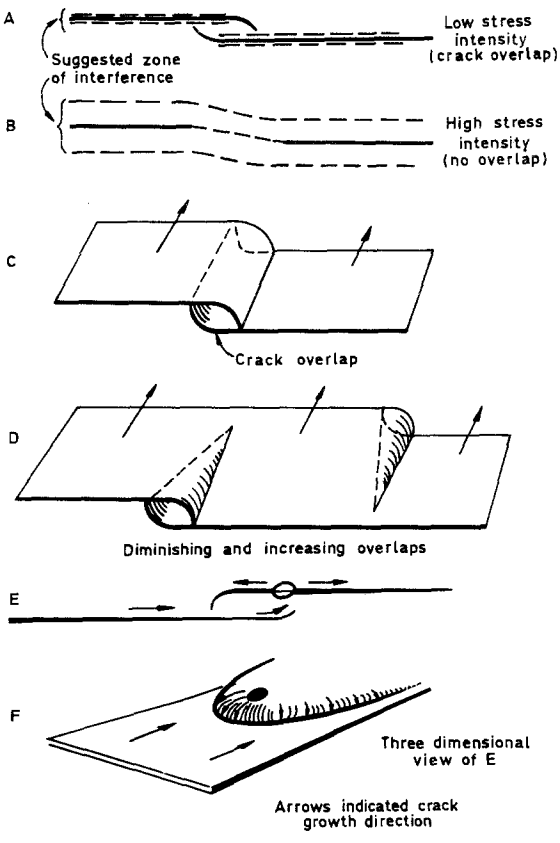

Figure 15 Schematic diagrams illustrating fatigue crack interactions – offset parallel cracks.

an arrangement of close proximity cracks [7], show that K_I rises abruptly when the tips are opposite one another, $a/b = 0.5$, and as they pass, K_{II} goes strongly negative for each tip which tilts them towards one another. The stress intensity falls dramatically and the cracks may not join until the crack front itself has driven forward far enough to raise it to complete the rupture process. This behaviour is always faithfully reproduced as the fracture mechanics solution would predict. However, the linear elastic solution cannot predict the change in behaviour as the stress is increased when the approaching segments now appear to deform and fuse into one another without a cliff being formed; Fig. 15 summarizes the observations. It is at this point that one must consider the effect of a continuum high strain deformation zone, or zone of interference, ahead and around the crack segment. Thus it seems that at low applied stresses, or where retardation is operating, zones are so small that for the offset in the segment level operative in the fatigue case they do not interact with their neighbours at a distance but the crack tips can pass one another before they respond, i.e. they behave as though the stresses were perfectly elastic.

It follows that, if under the most common fatigue loading conditions cracks grow completely under the influence of the maximum principal tensile stress, the mechanism of extension can be regarded as brittle fracture. The microstructural contribution can be seen to operate in two ways:

(i) by encouraging deviation of the crack onto easier crystallographic paths even though this results in tilting away from the normal plane, and

(ii) by encouraging steps or jogs to form along the crack front and thus fragmenting the plane of fracture. This second effect stems from the presence of particles and other imperfections.

These two separate contributions to the crack path deviation operate at different stages in crack growth. The crystallographic contribution is associated with low stress intensities (stage II growth) or under conditions where slip plane damage can accumulate (stage I growth). Contribution (ii) becomes stronger at higher stress intensities where particle fracture ahead or around the crack tip can occur, and particularly in regions of constraint. The result of this is that fatigue cracks may, as they grow, pass through a relatively planar growth phase [8] between the conditions under which the two mechanisms shown above are most active.

5. Conclusions

1. The periodic switching of load ratio (R) provides a clearly defined marking that enables crack growth behaviour to be followed back to about 10 μm from their origin.

2. Strong retardation effects have been observed in the low R period, up to 40 times.

3. The extent of the retardation zone has not yet been fully explored. No gradient in the striation spacing was observed in the retarded period although extending the number of cycles at low R gave a further increase in the retardation ratio.

4. The high R ratio growth rate as measured for short cracks in this switched programme seemed to be unaffected by the low R period inasmuch as the values obtained were in agreement with extrapolated long crack data.

5. The use of long crack data for life determinations for short cracks growing from holes would be acceptable for 7075-T7351 and 7010.

6. Both corner and bore fatigue origins have been encountered in this work. In general, peak

loads that raise the local stress at the hole to above yield result in bore origins and conversely stresses below yield promote corner cracks. This is in agreement with the findings in [9].

7. There was a tendency for cracks to grow somewhat faster along the bore of a hole than along the side. Consequently, corner cracks were not quite perfect quadrants. There was also a tendency for the crack front to be impeded along the bore surface zone so that a slight tunnelling effect could be observed. This could be practically eliminated by prior stress relief.

8. Fatigue cracks seem to interact with their neighbours in full accordance with fracture mechanics predictions, i.e. locally they behave as in a continuum. However there is also an influence of crystal structure, sharp tilts occurring in the general fracture plane when crossing grain boundaries.

Acknowledgements

This paper is published with the kind permission of the Copyright © Controller, HMSO, London, 1982.

References

1. MIL-A-83444 (US specification).
2. S. PEARSON, Fatigue crack initiation and propagation in half inch thick specimens of an aluminium alloy. RAE Technical Report 71109 (1971).
3. Engineering Sciences Data Unit, Fatigue crack propagation in aluminium plate, extruded bar and forgings. "Fatigue" Vol. 4, "Crack Propagation", Item No. 75029 (1975).
4. J. C. NEWMAN, Predicting failure of specimens with either surface cracks or corner cracks as holes. NASA TN D-8244 (1976).
5. T. T. SHIH and R. P. WEI, ASTM STP no. 595 (American Society for Testing and Materials, Philadelphia, 1976) p. 113.
6. C. A. STUBBINGTON, *Metallurgia* **68** (1963).
7. D. P. ROOKE and D. J. CARTWRIGHT, Compendium of stress intensity factors. Figs. 78 and 80. (HMSO, London, 1976).
8. P. J. E. FORSYTH and A. W. BOWEN, The relationship between fatigue crack behaviour and microstructure in 7178 aluminium alloy. RAE Technical Report 78006 (1978).
9. L. R. HALL and R. W. FINGER, Fracture and fatigue growth of partially embedded flaws. Proceedings of the Air Force Conference (1969). AFFDL Technical Report 70-144 (1970) pp. 235–62.

Received 18 October
and accepted 23 November 1982